

Hydrostatic equilibrium in a magnetized, warped Galactic disc

Andrew Fletcher and Anvar Shukurov^{*}

Department of Mathematics, University of Newcastle upon Tyne, NE1 7RU

Accepted 2001. Received 2001; in original form 2000

ABSTRACT

Hydrostatic equilibrium of the multiphase interstellar medium in the solar vicinity is reconsidered, with the regular and turbulent magnetic fields treated separately. The regular magnetic field strength required to support the gas is consistent with independent estimates provided energy equipartition is maintained between turbulence and random magnetic fields. Our results indicate that a midplane value of $B_0 = 4 \mu\text{G}$ for the regular magnetic field near the Sun leads to more attractive models than $B_0 = 2 \mu\text{G}$. The vertical profiles of both the regular and random magnetic fields contain disc and halo components whose parameters we have determined. The layer at $1 \lesssim |z| \lesssim 4 \text{ kpc}$ can be overpressured and an outflow at a speed of about 50 km s^{-1} may occur there, presumably associated with a Galactic fountain flow, if $B_0 \simeq 2 \mu\text{G}$.

We show that hydrostatic equilibrium in a warped disc must produce asymmetric density distributions in z , in rough agreement with HI observations in the outer Galaxy. This asymmetry may be a useful diagnostic of the details of the warping mechanism in the Milky Way and other galaxies. We find indications that gas and magnetic field pressures are different above and below the warped midplane in the outer Galaxy and quantify the difference in terms of turbulent velocity and/or magnetic field strength.

Key words: magnetic fields – MHD – ISM: magnetic fields – Galaxy: kinematics and dynamics – galaxies: ISM – galaxies: magnetic fields

1 INTRODUCTION

Models assuming hydrostatic equilibrium in the Galactic gas layer are often used to describe the global state of the interstellar medium (ISM) (Parker 1966, Badhwar & Stephens 1977, Bloemen 1987, Boulares & Cox 1990, Lockman & Gehman 1991, Kalberla & Kerp 1998). Despite matter outflows in the form of Galactic fountain (Shapiro & Field 1976, Bregman 1980, Habe & Ikeuchi 1980) and chimneys (Norman & Ikeuchi 1989), the assumption of hydrostatic equilibrium appears to be viable when considering the average state of the ISM over large scales or times. Korpi et al. (1999) argue that the warm ISM is on average in a state of equilibrium, although not the hot phase within $\simeq 1 \text{ kpc}$ from the midplane.

Magnetic fields play an important role in the pressure balance of the ISM (e.g. Parker 1979, Boulares & Cox 1990). Both theory and observations of interstellar magnetic fields assert that magnetic energy density should be comparable to turbulent and thermal energy densities of the gas (e.g.

Zweibel & McKee 1995, Beck et al. 1996), with a direct implication for a similar balance in the pressures.

The Galactic magnetic field has two distinct components, the regular field B on length scales of the order 1 kpc and the turbulent field b with a typical scale of order 100 pc . Galactic dynamo theory predicts that the strength of the regular field depends on magnetic diffusivity, rotational shear, the kinetic energy density of the ISM, etc. (Ruzmaikin, Sokoloff & Shukurov 1988, Ch. VII; Shukurov 1998). The turbulent magnetic field strength probably scales simply with the kinetic energy density of the turbulent gas (Beck et al. 1996, Subramanian 1999). Using the simplest form of this scaling in a model of the hydrostatic support of the ISM in the solar vicinity allows the pressure support from B and b to be separately quantified. In this paper we discuss implications, for the strength and vertical distribution, of both regular and turbulent magnetic fields, resulting from hydrostatic equilibrium models. The validity of the model is assessed using independent information on the magnetic fields in the ISM.

Descriptions of the state of the interstellar medium tend to concentrate on the situation in the solar vicinity. However, the gas disc is warped in the outer Galaxy (Binney

^{*} E-mails: andrew.fletcher@ncl.ac.uk and anvar.shukurov@ncl.ac.uk

1992), and the warping implies that there is an additional force involved in the vertical equilibrium balance. In Section 4 we use simple arguments to illustrate some effects of the warp on the vertical gas distribution and to suggest that the vertical gas distribution can have a characteristic asymmetry in the warped disc. Because of the warp, gas densities at ± 0.5 kpc above and below the displaced midplane can differ by a factor of 1.2. An asymmetry of this kind has been observed in the outer Galaxy (Diplas & Savage 1991), but went unnoticed.

2 HYDROSTATIC EQUILIBRIUM IN THE SOLAR NEIGHBOURHOOD

2.1 A model of hydrostatic support

We assume that, on average, the gas at the solar position is in a state of vertical hydrostatic equilibrium,

$$\frac{\partial P}{\partial z} = \rho g, \quad (1)$$

where P and ρ are the total pressure and gas density respectively, g is the gravitational acceleration and z is the height above the midplane. The assumption is probably weakest when considering the hot, ionized gas which presumably originates in the disc but fills the Galactic halo, and so is involved in systematic vertical motions. However, hydrostatic equilibrium is still a plausible expectation for large areas, of order a few kiloparsecs in size.

The equilibrium model includes several contributions to the total pressure,

$$P = P_g + P_m + P_{cr},$$

with

$$P_g(z) = \sum_i \rho_i v_{zi}^2 + \sum_i n_i k T_i$$

the gas pressure consisting of the turbulent and thermal components (with contributions from individual phases of the ISM labelled with index i), P_m the magnetic pressure due to the regular, B , and random, b , magnetic field components, and P_{cr} the cosmic ray pressure. Here v_{zi} is the vertical component of the rms turbulent velocity in the i 'th phase, n_i the gas number density, T_i the temperature and k is Boltzmann's constant.

We separate the pressure due to the regular and turbulent magnetic fields by assuming that the energy density of the turbulent magnetic field is a multiple of the kinetic energy density of the turbulent gas,

$$P_m = \frac{B^2 + b^2}{8\pi}, \quad \frac{b^2}{8\pi} = \frac{1}{2} K \sum_i \rho_i v_i^2, \quad (2)$$

with K a constant and $v_i^2 = 3v_{zi}^2$ is the total turbulent velocity. A value of $K \simeq 1$ is in line with theoretical arguments showing that equipartition should exist between turbulent kinetic energy and magnetic energy densities (Zweibel & McKee 1995, Beck et al. 1996). If the turbulent magnetic field is concentrated into flux ropes and within these ropes energy equipartition also exists (Subramanian 1999), then K is the filling factor of the ropes.

By taking \mathbf{B} to be parallel to the Galactic plane we neglect the contribution of magnetic tension due to the regular

Table 1. Gas components of the modelled ISM at the solar position

Component	n_0 cm ⁻³	h pc	T K	v_z km s ⁻¹
Molecular ^(a)	0.3	70	20	4.5
Cold ^(a)	0.3	135	100	6
Warm ^(a)	0.1	400	8×10^3	9
Diffuse ionized ^(b)	2.4×10^{-2}	950	8×10^3	12
Halo, ionized ^(c)	1.2×10^{-3}	4400	1.5×10^6	60
Halo, neutral ^(d)	1.3×10^{-3}	4400	10^4	60

Midplane number density n_0 , scale height h , temperature T and one-dimensional turbulent velocity dispersion v_z for the ISM components are given at the solar position. All components are assumed to have a Gaussian distribution except the halo gas, which is taken to have an exponential distribution. References: (a) Bloemen (1987), (b) Reynolds (1990a), (c) Pietz et al. (1998), (d) Kalberla et al. (1998).

field to the support of the ISM (cf. Boulares & Cox 1990). The vertical regular magnetic field is definitely negligible near the midplane away from the disc centre (Ruzmaikin et al. 1988, Beck et al. 1996). The dominance of the horizontal magnetic field is more questionable in the Galactic halo. Significant vertical magnetic fields have been detected in the haloes of only two galaxies with strong star formation (NGC 4631, Hummel et al. 1988, 1991 and M82, Reuter et al. 1994), but the Milky Way hardly belongs to this type. Vertical dust filaments abundant in many galaxies in the disc-halo interface (Sofue 1987) may indicate significant localized vertical magnetic fields there. These can be a result of shearing the horizontal field in the disc by a galactic fountain and/or chimneys (cf. Korpi et al. 1999; see also Elstner et al. 1995). Still, this interpretation is compatible with a predominantly horizontal regular magnetic field in the main parts of both the disc and the halo away from the interface (e.g. in M51 – Berkhuijsen et al. 1997). In the absence of direct observational evidence for the halo of the Milky Way, we refer to numerous theoretical models which invariably indicate the dominance of the horizontal regular magnetic field under a variety of physical setups (e.g. Brandenburg et al. 1992, 1993; Brandenburg, Moss & Shukurov 1995).

The ISM has a multicomponent structure; parameters of the basic phases are given in Table 1. Molecular hydrogen, together with the cold and warm neutral phases make up the bulk of the gaseous disc mass, the other components being the diffuse ionized gas (also known as the Reynolds layer), a neutral halo and ionized halo gas (Ferrière 1998, Kalberla & Kerp 1998). Different phases do not necessarily have a distinct physical nature and the distinction is often merely conventional; for example, neutral and ionized halo components plausibly represent a single physical entity; likewise, the separation of the warm and diffuse ionized phases may simply describe the increase of ionization degree with height. The halo components are present in the disc as the hot phase. The filling factor for them was taken to be that of the hot phase, 0.3 in the midplane, rising to 0.9 at $z = 4$ kpc and 1 further up in the halo, in an approximation to Fig. 10 of Ferrière (1995) (see also Rosen & Bregman 1995, Korpi et al. 1999). To allow for helium, nine percent by number of hydrogen atoms has been added to obtain the mass density in each phase, and we assume that the helium is fully ionized in the ionized halo component.

We note that observational estimates of the total random velocity in the diffuse ionized gas yield supersonic values 20 km s^{-1} (Reynolds 1990a). This can be due to systematic (albeit random) upward motions of the hot gas forming the base of the galactic fountain (cf. Korpi et al. 1999) rather than to genuine turbulent motions; the ram pressure of these motions contributes to the vertical support of the gas and we can include it in the turbulent pressure.

The pressure of cosmic rays is assumed to be equal to that of the total magnetic field, $P_{\text{cr}} = P_{\text{m}}$ where P_{m} is given by Eq. (2). Altogether, the total pressure is given by

$$P = (3K + 1) \sum_i \rho_i v_{zi}^2 + \sum_i n_i k T_i + \frac{B^2}{4\pi}. \quad (3)$$

2.2 Observational constraints on magnetic field near the Sun

The vertical distribution of B is poorly known, and we derive it in Section 3 from Eqs (1) and (3), and then assess the validity of our results using the following reasonably well established constraints.

First, if equipartition between the energy densities of cosmic rays and magnetic fields is assumed then the total interstellar magnetic field, $B_{\text{tot}} = \sqrt{B^2 + b^2}$, at $z = 0$ is estimated from synchrotron intensity as $B_{\text{tot}} \simeq 6 \mu\text{G}$ (Beck 2001). With observations of synchrotron polarization showing $B_0/B_{\text{tot}} \simeq 0.6$, as described below, this gives $B_0 \simeq 4 \mu\text{G}$ (Beck 2001); if anisotropic turbulent magnetic fields are present this is an upper limit on B_0 . Observations of Faraday rotation measures from pulsars and extragalactic radio sources yield a midplane value of B of $B_0 \simeq 2 \mu\text{G}$ (Rand & Kulkarni 1989, Lyne & Smith 1989, Rand & Lyne 1994, Frick et al. 2001). Note that B_0 can be significantly larger at a distance of a few kiloparsecs from the Sun because the Sun is located close to a reversal of the large-scale magnetic field (e.g. Beck et al. 1996). Magnetic field strengths obtained from rotation measures can be underestimated if the ISM is in pressure balance, so B and ρ are anti-correlated (Beck 2001). Therefore we consider models with B_0 equal to $4 \mu\text{G}$ and $2 \mu\text{G}$.

Second, the ratio of the turbulent to regular magnetic field, b/B , is directly related to the degree of polarization, \mathcal{P} , of the Galactic synchrotron emission via $\mathcal{P} = \mathcal{P}_0 B^2 / (b^2 + B^2)$ with $\mathcal{P}_0 \approx 0.7$, provided any depolarization effects can be neglected (Burn 1966, Sokoloff et al. 1998). Berkhuijsen (1971) found $b/B \simeq 1.2$ and Philipps et al. (1981) argue that b/B cannot be much larger than unity. Observations of the Galactic polarized synchrotron background yield $1 \lesssim b/B \lesssim 3$ (Spoelstra 1984). This is corroborated by analyses of Faraday rotation measures of extragalactic radio sources and pulsars which imply $b/B \simeq 1.7$ (Ruzmaikin et al. 1988, Ch. IV and references therein) and $b/B \simeq 3$ (Rand & Kulkarni 1989) (these are upper limits if B is underestimated).

Finally the vertical distribution of the total interstellar magnetic field, can be obtained from the distribution of Galactic synchrotron emission (Phillips et al. 1981, Beuermann, Kanbach & Berkhuijsen 1985). The model used by Phillips et al. (1981) requires halo emissivity of about 10 percent of that in the disc, extending to about 10 kpc beyond the midplane. Roughly, emissivity is proportional to

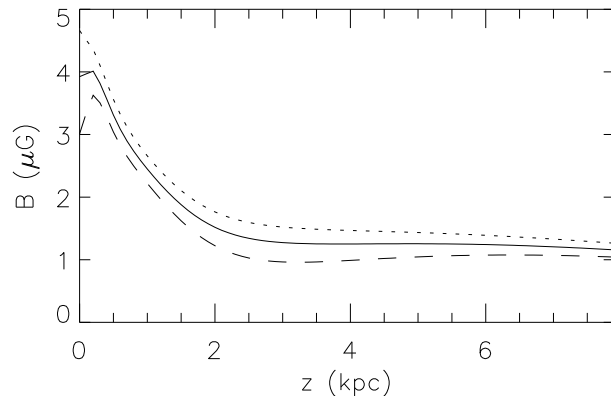


Figure 1. The regular magnetic field, B , required for precise hydrostatic equilibrium with a midplane strength $B_0 \simeq 4 \mu\text{G}$, for $K = 0.8$ (solid), $K = 0.6$ (dotted) and $K = 1.0$ (dashed), where K is the ratio of turbulent magnetic to kinetic pressures defined in Eq. (2).

the total magnetic field squared or to a higher power if detailed equipartition between magnetic fields and cosmic rays is maintained (Beck et al. 1996, Zweibel & Heiles 1997, Sokoloff et al. 1998). So the total magnetic field, B_{tot} , in the halo is expected to be approximately $1/3$ – $1/2$ of that in the disc, $B_{\text{tot}}(\text{halo})/B_{\text{tot}}(\text{disc}) = 1/3$ – $1/2$.

3 THE ROLE OF MAGNETIC FIELD IN THE SUPPORT OF THE GAS LAYER

The vertical distribution of the interstellar magnetic field is even more difficult to obtain from observations than that of the gas components of the ISM. Therefore we obtain B as a function of z from a hydrostatic equilibrium model and then compare the result with independent information briefly summarized above. This also allows us to reassess the validity of the equilibrium model itself.

Equation (1), with P from Eq. (3), is solved for $B(z)$ using different values of K . We use g for the solar vicinity derived by Ferrière (1998) from Kuijken & Gilmore (1989a,b),

$$-g = A_1 \frac{z}{(z^2 + Z_1^2)^{1/2}} + A_2 \frac{z}{Z_2}, \quad (4)$$

where $A_1 = 4.4 \times 10^{-9} \text{ cm s}^{-2}$, $A_2 = 1.7 \times 10^{-9} \text{ cm s}^{-2}$, $Z_1 = 0.2 \text{ kpc}$ and $Z_2 = 1 \text{ kpc}$.

3.1 Model with $B_0 \simeq 4 \mu\text{G}$

Constraining the midplane regular magnetic field to $B_0 \simeq 4 \mu\text{G}$, as suggested by cosmic ray energy equipartition arguments (Beck 2001), we obtain the vertical distributions of B and b shown in Figs 1 and 2. The best fit to all three constraints described in section Section 2 is with $K = 0.8$, in line with theoretical equipartition arguments (Zweibel & McKee 1995, Beck et al. 1996); we obtain $B_0 = 4 \mu\text{G}$, $b/B = 1.25$ at $z = 0$ and $B_{\text{tot}}(\text{halo})/B_{\text{tot}}(\text{disc}) \simeq 1/3$.

Increasing K amplifies the contribution of the turbulent magnetic field and cosmic rays to the equilibrium balance, according to Eq. (2). Near the midplane, the strong turbulent pressure (kinetic and magnetic) created by molecular

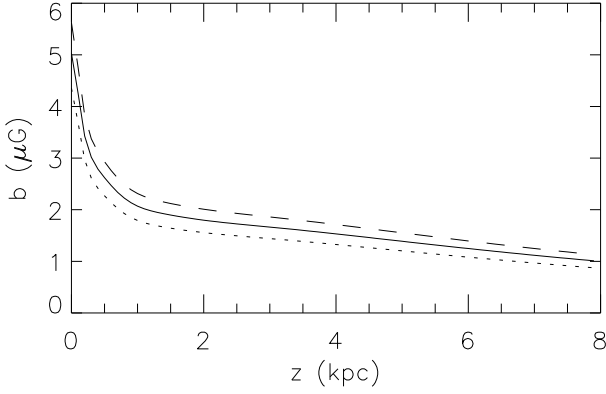


Figure 2. Turbulent magnetic field strength, b , for the model of Fig. 1 (with $B_0 \simeq 4 \mu\text{G}$) for $K = 0.8$ (solid), $K = 0.6$ (dotted) and $K = 1.0$ (dashed).

cloud motions is amplified to such an extent that the required strength of the regular magnetic field for hydrostatic equilibrium begins to drop as K increases (see the solid and dashed lines in Fig. 1) reaching zero for $K = 1.4$.

Figure 1 suggests a two-component model of $B(z)$, a disc with a scale height of $h_B \simeq 1$ kpc and a halo extending $z \simeq 10$ kpc with a roughly constant field strength of $B \simeq 1 \mu\text{G}$. The scale height of the diffuse ionized gas (Table 1) is roughly the same as h_B . This is also in good agreement with Han and Qiao (1994) who have estimated $h_B \simeq 1.2$ kpc from Faraday rotation measures of extragalactic radio sources. Polarized radio emission, indicating the presence of a regular magnetic field, has been detected high in the haloes of the edge-on spiral galaxies to $z \simeq 4$ kpc in NGC 891 and to $z \simeq 8$ kpc in NGC 4631 (Hummel, Beck & Dahlem 1991).

Figure 2 shows a similar two-component structure of the turbulent magnetic field b ; a disc with scale height of $h_b \simeq 0.5$ kpc and a slowly varying field in an extended halo (with b decreasing by a factor of two at $z \approx 7$ kpc), where $B \simeq b$. We note a significant difference between the scale heights of the regular and turbulent magnetic fields, $h_B/h_b \simeq 2$ for the narrower components. This may have important implications for theories of galactic magnetic fields.

3.2 Model with $B_0 \simeq 2 \mu\text{G}$

If B_0 is significantly smaller than $4 \mu\text{G}$ then the best fit to the constraints described in Section 2 is with $K = 1.6$ (Figs 3 and 4); we obtain $B = 2.4 \mu\text{G}$ at the midplane (but excluding the molecular gas; see the discussion in Section 3.2.2), $b/B \approx 2.4$ and $B_{\text{total}}(\text{halo})/B_{\text{total}}(\text{disc}) \approx 1/3$. Realistic variations of the gas parameters do not produce outcomes meeting all three criteria far from $K = 1.6$, which results in a constraint $1.5 \lesssim K \lesssim 1.7$. Using a different representation of g for the stellar disc derived by Rohlfs (1977, p.35), with gravity from a spherical dark matter halo added as $V_{\text{tot}}^2 z/R_\odot$, where V_{tot} is the rotation speed of the disc and R_\odot the solar radius, the range becomes $1.3 \lesssim K \lesssim 2.4$. If K is beyond this range, then either $B_0 > 3 \mu\text{G}$, or $B_0 < 1 \mu\text{G}$, or $b_0/B_0 > 3$ must be accepted for the midplane values.

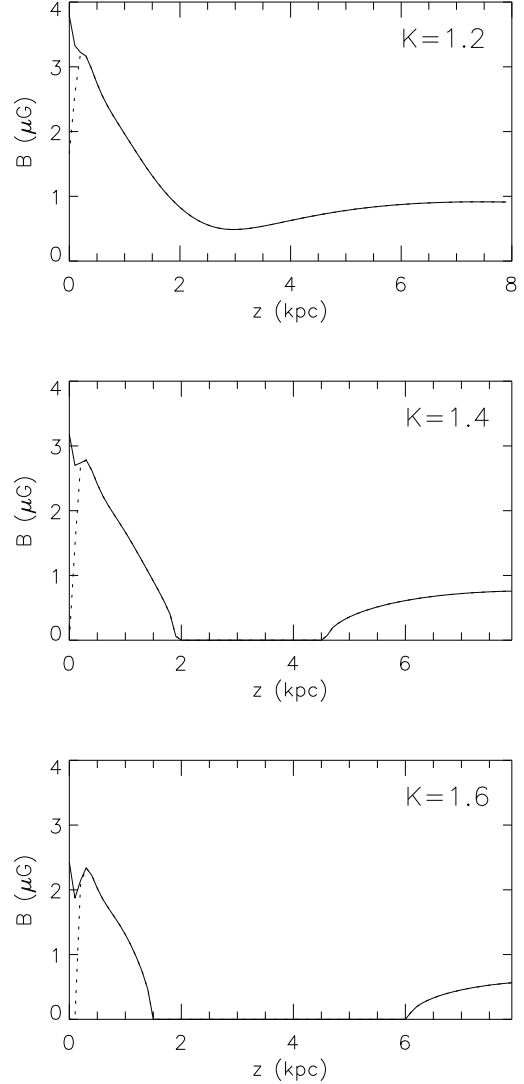


Figure 3. The regular magnetic field, B , required for precise hydrostatic equilibrium with a midplane strength $B_0 \simeq 2 \mu\text{G}$, for different values of K with both the pressure and mass contributions from molecular clouds omitted (solid line) and with the molecular clouds included (dotted line up to $z \simeq 0.2$ kpc, solid line above). In those ranges of z where $B = 0$, the hydrostatic equilibrium equations formally require negative magnetic pressure thereby indicating an overpressured region.

3.2.1 Overpressure above $z \simeq 1$ kpc

A strange feature of Fig. 3, for the better fits at $K = 1.4$ and 1.6, is the apparent absence, or a strong decrease, of B at $z = 1$ –6 kpc. The reason for this is clear from Fig. 5; where we show the total pressure excess over the hydrostatic equilibrium value,

$$\Delta P = P - \int_z^\infty \rho g dz, \quad (5)$$

assuming $B(z)$ is as in Fig. 3 but not less than $1 \mu\text{G}$ at any z . We see that there is more than enough pressure from the gas, turbulent magnetic field and associated cosmic rays to support the weight of the overlying ISM at $1 \lesssim z \lesssim 6$ kpc.

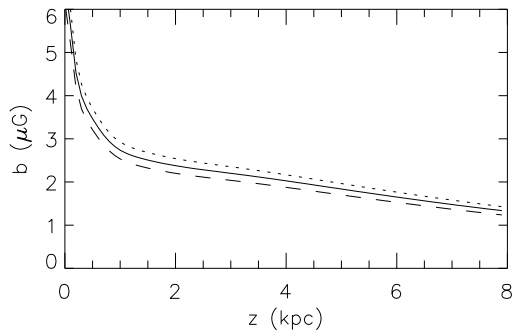


Figure 4. Turbulent magnetic field strength, b for the model with $B_0 \simeq 2 \mu\text{G}$, excluding the effect of molecular cloud turbulent energy, for $K = 1.2$ (dashed), $K = 1.4$ (solid) and $K = 1.6$ (dotted).

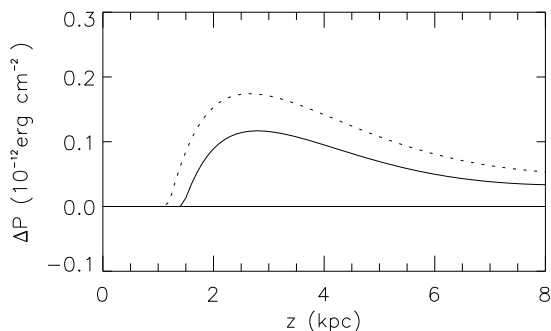


Figure 5. Pressure excess over the hydrostatic equilibrium value, described by Eqs. (3) and (5), using B shown in Fig. 3 but with minimum of B enforced to be $1 \mu\text{G}$, for $K = 1.4$ (solid) and $K = 1.6$ (dashed). Positive ΔP indicates overpressure.

Any further contribution from the regular magnetic field enhances overpressure in this range of z .

The excess pressure at $z = 1\text{--}4$ kpc, if real, apparently contributes to driving the Galactic fountain flow. The vertical velocity driven by the overpressure is $V_z \simeq (\frac{1}{2}\Delta P/\rho)^{1/2} \simeq 50 \text{ km s}^{-1}$, significantly smaller than the magnetosonic speed (100 km s^{-1} or more) and compatible with what can be expected for galactic fountains. It is notable that a similar systematic outflow of the hot gas occurs in models of multiphase ISM driven by supernovae (Rosen & Bregman 1995, Korpi et al. 1999, Shukurov 1999).

3.2.2 Molecular clouds

An unsatisfactory feature of the distribution shown with the dotted line in Fig. 3 (i.e. for a model including the molecular gas) is the deep minimum of B at $z = 0$. This feature also occurs in the model of Boulares & Cox (1990, their Fig. 2). It is very unlikely that B can have such a sharp minimum even if it has a global odd parity in z , resulting in the constraint $B_0 = B(0) \equiv 0$. Apart from increasing B_0 to $4 \mu\text{G}$ (Section 3.1), a possible resolution of this difficulty assumes that the coupling between kinetic energy density and turbulent magnetic fields, parameterized by K , is weaker for the bulk

motion of molecular clouds than for other ISM phases. This assumption is physically compelling because the clouds represent the densest, self-gravitating part of the ISM, rather isolated from the other diffuse phases. The minimum in B does not occur if $K \lesssim 0.5$ for the molecular clouds and $K \simeq 1$ in the other phases. If, otherwise, $K \simeq 1$ for the bulk motion of molecular clouds as well, then either B must grow sharply in the range $|z| < 100$ pc from a small midplane value, or $B > 3 \mu\text{G}$ at $z = 0$ (cf. the upper panel of Fig. 3).

A possible interpretation is that the turbulent magnetic field interacts differently with the molecular clouds than with the diffuse phases of the ISM (e.g. because of the fluctuation dynamo action in the diffuse gas – see Sect. 4.1 in Beck et al. 1996 and Subramanian 1999). If the fractional volume swept by the molecular clouds over the correlation time of b is significantly less than unity, only a correspondingly small fraction of the magnetic field will be coupled to the clouds. The number of clouds in a correlation volume l^3 of the turbulent magnetic field is $N \simeq (l/l_c)^3 f_c$, where f_c is the volume filling factor of the clouds and l_c is the cloud size. During the correlation time of the magnetic field, $\tau \simeq l/v$, the clouds moving at a speed $v_c \approx 8 \text{ km s}^{-1}$ (cf. Table 1) sweep the volume $V \simeq N l_c^2 v_c \tau$. So the clouds affect magnetic fields within the fractional volume $V/l^3 \simeq f_c v_c l / (v l_c)$, where v is the r.m.s. turbulent velocity in the ambient medium. With $f_c = 10^{-3}\text{--}10^{-4}$ (Berkhuijsen 1999 and references therein), $l/l_c \simeq 10$ and $v/v_c \simeq 2$, we obtain $V/l^3 \simeq 5 \times (10^{-2}\text{--}10^{-3}) \ll 1$, so the coupling between molecular clouds and the intercloud magnetic fields is expected to be weak. Molecular clouds move with respect to the surrounding gas, so their connection with the external magnetic field can be lost rapidly. Equipartition can still be maintained within the clouds but may not occur between the bulk motion of the clouds (that provides the average pressure support to the ISM) and the turbulent magnetic field.

The same arguments apply to the regular magnetic field and one might expect a relatively weak dependence of B on the parameters of the molecular gas (cf. Beck 1991). We show in Fig. 4 the vertical profile of the turbulent magnetic field b calculated from Eq. (2) for a choice of K values, where the contribution of molecular clouds to kinetic energy density has been suppressed. With the contribution of molecular gas to b suppressed in Eq. (2), the turbulent magnetic field is reduced near $z = 0$ giving room for a stronger regular magnetic field. The scale height h_b is not sensitive to different values of K .

3.3 Equilibrium near the Sun: discussion

The comparative simplicity of the results obtained with $B_0 \simeq 4 \mu\text{G}$, compared to those discussed in Section 3.2 for weaker B_0 , as well as their quantitative and qualitative plausibility leads us to favour the arguments suggesting $B_0 \simeq 4 \mu\text{G}$ in the solar vicinity.

The results of our model with $B_0 \simeq 4 \mu\text{G}$, discussed in Section 3.1, compare reasonably well with the vertical distribution of the magnetic field derived by Kalberla & Kerp (1998, K&K hereafter) using a hydrostatic equilibrium model, shown in their Fig. 5. In particular, K&K predict a regular magnetic field in the halo of $B \simeq 1 \mu\text{G}$ at $z \simeq 8$ kpc as a requirement for hydrostatic equilibrium. However, K&K have a weaker turbulent magnetic field, with $b_0 \simeq 3.5 \mu\text{G}$,

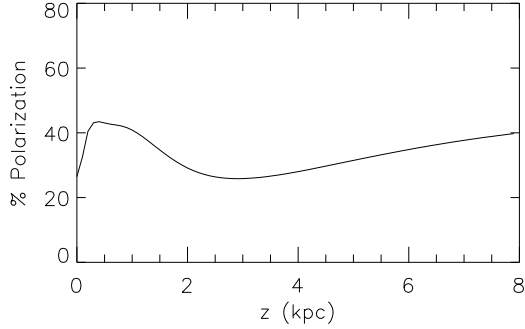


Figure 6. Expected percentage polarization of non-thermal radio emission, using the regular and turbulent magnetic field distributions from Figs 1 and 2 (for $K = 0.8$) in Eq. (6), with $\mathcal{P}_0 = 70\%$.

that extends to only $z \simeq 2$ kpc compared to $z > 8$ kpc in our model. Polarized radio emission from the haloes of the edge-on spiral galaxies NGC 891 and NGC 4631 is significantly depolarized by turbulent magnetic fields (Hummel et al. 1991) and any large scale fields present in the halo must become tangled by turbulence and Parker and thermal instabilities (Beck et al. 1996), so we expect to see a turbulent component of the magnetic field at all z .

In contrast to K&K, who have magnetic pressure in the disc of 1/3 the total gas pressure and no pressure contribution from cosmic rays, we find equality between the gas (turbulent plus thermal) and total magnetic field pressures in the region $|z| < 1$ kpc. And whereas K&K have pressure equilibrium between gas and magnetic fields in the halo at $z \simeq 5$ kpc our model only requires $P_m \simeq 0.5P_g$. We have assumed equipartition between cosmic ray and magnetic pressures at all z .

3.3.1 Implications for external galaxies

The observed degree of linear polarization of synchrotron radio emission is given by Burn (1966) as

$$\mathcal{P} = \mathcal{P}_0 \frac{B_{\perp}^2}{B_{\perp}^2 + b_{\perp}^2}, \quad (6)$$

where B_{\perp} and b_{\perp} are, respectively, the regular and turbulent (isotropic) magnetic field components transverse to the line of sight and $\mathcal{P}_0 \approx 70\%$ is the degree of polarization in a purely regular field. Assuming that $b_{\perp}^2/B_{\perp}^2 \simeq b^2/B^2$ Fig. 6 shows the expected variation in \mathcal{P} with z .

An implicit assumption in Fig. 6 is that \mathcal{P}_0 is constant in z . However, $\mathcal{P}_0 = (\gamma + 1)/(\gamma + \frac{1}{3})$ depends on the electron energy spectral index γ . If γ increases with z , due to cosmic ray electron energy losses as they travel into the halo, then \mathcal{P}_0 and hence \mathcal{P} will increase with z making the slope at $z \gtrsim 3$ kpc in Fig. 6 even steeper, although this effect is only weak.

Observations of polarized radio emission from edge-on galaxies, such as NGC 891 (Hummel et al. 1991, Dumke et al. 1995) and NGC 4631 (Hummel et al. 1991, Golla & Hummel 1994, Dumke et al. 1995) show the degree of polarization rising with z from a minimum at $z = 0$. The observed small \mathcal{P} at the midplane, e.g. $\mathcal{P}|_{z=0} \simeq 1\%$ in NGC 891 (Hummel et al. 1991), can be explained by strong Faraday

depolarization by both regular and turbulent fields in the disc. Above $z \simeq 2$ kpc, the steady increase in \mathcal{P} shown in Fig. 6 is reproduced in the observations, but \mathcal{P} in Fig. 6 is a factor of two higher than observed in external galaxies at the wavelength $\lambda = 20$ cm. Faraday depolarization due to both regular and turbulent magnetic fields is expected to be weak in galactic halos where Faraday rotation measure does not exceed 10 rad m^{-2} due to low gas density. For example, depolarization by internal Faraday dispersion arising from a turbulent magnetic field $b \simeq 2 \mu\text{G}$ with correlation length $l \simeq 0.5$ kpc (Poezd, Shukurov & Sokoloff 1993), path length through the halo $L \simeq 10$ kpc and thermal electron density $n_e \simeq 10^{-3} \text{ cm}^{-3}$ can only reduce the degree of polarization by a few percent even at $\lambda = 20$ cm, $\mathcal{P} = \mathcal{P}_0(1 - e^{-S})/S \approx 0.96\mathcal{P}_0$, where $S = 4\lambda^4(0.81n_e b)^2 L L$ (Burn 1966, Sokoloff et al. 1998).

A plausible explanation of the relatively low polarization of synchrotron emission from galactic halos of edge-on galaxies is that b_{\perp}^2/B_{\perp}^2 is larger ($\simeq 6$) than predicted by our model (2–3) for the Milky Way.

4 HYDROSTATIC EQUILIBRIUM IN THE OUTER GALAXY

The Galactic gas disc is warped beyond the solar orbit (Binney & Tremaine 1987, Binney 1992). The warp is thought to propagate through the disc in azimuth and the speed of propagation determines whether the ISM at large radii has enough time to reach a state of hydrostatic equilibrium. The period of the warping wave is about 3×10^8 yr, assumed to be similar to the disc rotation period at a radius 12 kpc where the warp starts (Binney 1992). This is longer than the sound crossing time over a scale height of 1 kpc at the sound speed of 10 km s^{-1} . Thus, hydrostatic equilibrium can be a valid first approximation for the state of the gas at $R = 12$ – 18 kpc (see, however, Masset & Tagger 1996, for a discussion of possible deviations from equilibrium).

In this section we argue that the warping can lead to a noticeable asymmetry in the vertical profile of the gas density and confirm this using the vertical H I distributions in the outer Galaxy obtained by Diplas & Savage (1991).

We describe positions in Galactocentric polar coordinates (R, Θ, z) , where R is distance in the Galactic plane from the Galactic centre, Θ is the azimuth in the Galactic plane, with the Sun at $\Theta = 180^\circ$ and Θ increasing anticlockwise viewed from the north Galactic pole; and z is vertical distance from the Galactic plane. The galactocentric distance of the Sun is adopted as $R_{\odot} = 10$ kpc, rather than the currently used $R_{\odot} = 8.5$ kpc to avoid the need to rescale the data of Diplas & Savage (1991).

4.1 The observed vertical asymmetry in H I density

Data from the northern hemisphere H I survey (Stark et al. 1991) was used by Diplas & Savage (1991) to study the gas morphology in the outer Galaxy. The data show a distinct asymmetry in the vertical distribution of H I across a substantial region of the outer disc. The asymmetry can also be seen, but less distinctly, in maps of the outer Galaxy presented by Burton (1988, Fig. 7.18).

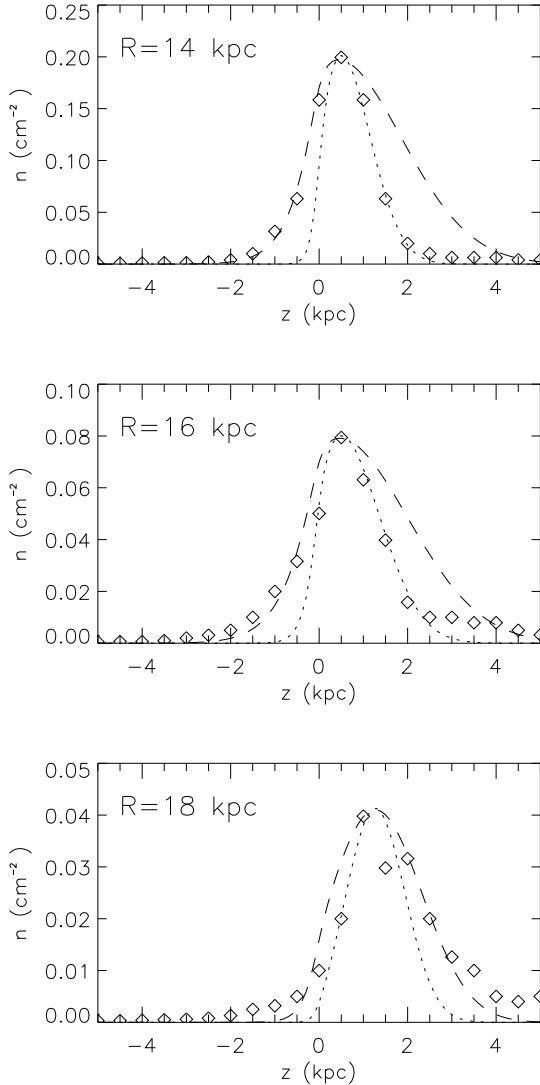


Figure 7. H I number density from Diplas & Savage (1991) at various R and $\Theta = 90^\circ$ (diamonds) and fits using two different velocity dispersions in a warped gas disc with the asymmetric gravity of Fig. 8. Dashed: $u = 7, 8$ and 5 km s^{-1} from top to bottom. Dotted: and $u = 15, 15$ and 8 km s^{-1} from top to bottom.

The asymmetry occurs over a sector of the outer Galactic disc in the azimuthal range $\Theta = 60^\circ$ to $\Theta = 110^\circ$, visible between $R = 14$ and 18 kpc . It is notable that the warping is maximum in this region (Diplas & Savage 1991). Unfortunately, the region around $\Theta = 270^\circ$ where the other crest of the warp is located is not accessible for a northern hemisphere survey.

Diplas & Savage (1991) do not comment directly on the asymmetry, but the data reduction process used can lead to some mis-positioning of gas, especially at lower densities, because of confusion with H I clouds moving with peculiar velocities. (B. Savage, 1998, private communication). Reversing the calculations of Diplas & Savage (1991) in the region of asymmetry shows that the velocity of the H I, $-100 < v < -40 \text{ km s}^{-1}$, is indeed similar to that of intermediate velocity clouds (Wesselius & Fejes 1973, Kuntz

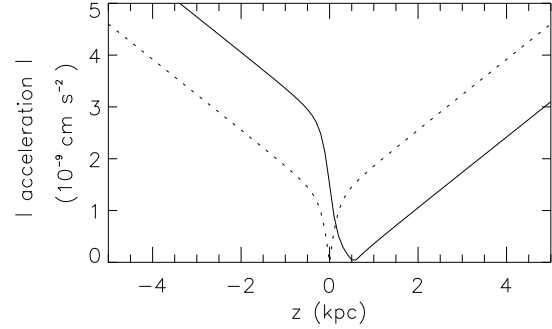


Figure 8. The vertical acceleration in a warped disc. Radial extrapolation, to $R = 16 \text{ kpc}$, of the acceleration due to gravity from the solar position after Ferrière (1998), $|g|$ from Eq. (8) (dotted) and $|g + a_0|$ with constant a_0 added to move the minimum to $z = 0.5 \text{ kpc}$ in a rough model of the force responsible for the warp (solid).

& Danly 1996). However the region ($35^\circ \lesssim l \lesssim 78^\circ$ and $-8^\circ \lesssim b \lesssim 8^\circ$, where l and b are Galactic longitude and latitude) is too large to be associated with a single cloud. We proceed with the assumption that the asymmetry is a real feature of the outer Galaxy gas distribution.

The results of Diplas & Savage (1991), for three positions in the outer Galaxy, are illustrated in Fig. 7. The maximum gas density is displaced to positive z , reflecting the warp of the gas disc. It is also clear that the gas density is asymmetric with respect to the displaced midplane, with a density excess at positive z .

4.2 Asymmetry in the vertical H I density caused by the warp

To model gas equilibrium in a warped disc, we describe the warp locally as being produced by a z -independent acceleration a_0 , added across all z as required to make $z = 0.5 \text{ kpc}$ the bottom of the potential well. Since the stellar disc is not significantly warped, we scaled g of Eq. (4) to the outer Galaxy (Ferrière 1998) (neglecting edge effects and gravity from the gas since the region of interest is not far from the edge of the stellar disc) and then added a constant acceleration $a_0 = 1.5 \times 10^{-9} \text{ cm s}^{-2}$ at $R = 16 \text{ kpc}$. The modulus of the resulting vertical acceleration is shown in Fig. 8. Acceleration of this magnitude displaces the gas density maximum to the observed height at this radius. Thus, the vertical equilibrium equation (1) is replaced by

$$\frac{\partial P}{\partial z} = \rho(g + a_0), \quad (7)$$

with

$$-g = \frac{A_1 z}{\sqrt{z^2 + Z_1^2}} \exp\left(-\frac{R - R_\odot}{R_1}\right) + A_2 \frac{z}{Z_2} \frac{R_\odot^2 + R_2^2}{R^2 + R_2^2}, \quad (8)$$

where A_1 , A_2 , Z_1 and Z_2 are defined after Eq. (4) and $R_1 = 4.9 \text{ kpc}$, $R_2 = 2.2 \text{ kpc}$.

If all of the pressure sources are symmetric with respect to the shifted midplane, the asymmetric force of Eq. (7) should give rise to a larger gas scale height above the shifted

midplane at 0.5 kpc, similar to what is observed – see fits in Fig. 7.

To further, investigate the effect of the warp, we use Parker’s (1966) model of hydrostatic equilibrium

$$\rho(z) = \rho_0 \exp \left[\frac{-\Phi(z)}{(1 + \alpha + \beta)u^2} \right], \quad (9)$$

where Φ is the gravitational potential, obtained by integrating Eq. (8) and α and β represent the pressures due to magnetic fields and cosmic rays, respectively, as multiples of the gas pressure. A more detailed analysis as in Section 2 is hardly warranted here because of our limited knowledge of the gas parameters in the outer Galaxy. Assuming $\alpha = \beta = 1$ and using the asymmetric force of Eq. (7), we fitted Eq. (9) to the observed density distribution using different values of the effective total gas velocity dispersion, u .

As shown in Fig. 7, the density distributions are reproduced satisfactorily close to the shifted midplane with a single (smaller) velocity dispersion. However, there is additional asymmetry at larger heights which can be accounted for by larger values of u at negative z , at least at $R = 14$ and 16 kpc. The same effect is found at other positions in the sector of the Galactic disc that is positively warped; at each position a further source of asymmetry is required as a higher order effect at large heights.

To quantify deviations from Eq. (7) with a constant a_0 , we show in Fig. 9 the residual acceleration

$$a_1 = \rho^{-1} \frac{\partial P}{\partial z} - g - a_0,$$

at $R = 16$ kpc both for a uniform velocity dispersion $u = 11.5 \text{ km s}^{-1}$, a mean between the two approximations of Fig. 7, and for $u = 8 \text{ km s}^{-1}$ (shown dotted in Fig. 7) above the shifted midplane and $u = 15 \text{ km s}^{-1}$ (dashed in Fig. 7) below the midplane. The residual, asymmetric component of the acceleration is $|a_1| \simeq 10^{-9} \text{ cm s}^{-2}$ or less at $\Delta z = \pm 1$ kpc from the midplane of the warped disc, so $|a_1/a_0| < 0.7$.

The former option, illustrated in Fig. 9a, attributes the whole residual asymmetry to a z -dependent component of the warping force, a_1 , which then must vary at a scale of order 1 kpc, with a_1 possibly becoming comparable to a_0 at large heights.

In the latter case, illustrated in Fig. 9b, one supposes that a part of the residual asymmetry is due to an asymmetric pressure in the ISM. We have quantified the residual in terms of velocity dispersions. An obvious candidate for the residual asymmetry can be the regular magnetic field $B(z)$. We note that some galactic dynamo models are compatible with strongly asymmetric $B(z)$ where $B(z)$ vanishes in a layer at a height of about 1 kpc on one side of the disc. This could happen if regular magnetic fields in the disc and halo have different parities in z (Sokoloff & Shukurov 1990, Brandenburg et al. 1992). The range of a_1 in Fig 9b, Δa_1 , would correspond to an asymmetric component of $B(z)$ of order $\sqrt{\rho \Delta a_1 \Delta z} \simeq 1 \mu\text{G}$, where $\Delta a_1 \simeq a_1$, gas density corresponds to 0.03 cm^{-3} , and B has to be smaller above the midplane $z > 0$.

5 SUMMARY

As discussed in Section 3, parameters of a multiphase ISM in the solar vicinity are compatible with a model of hydrostatic

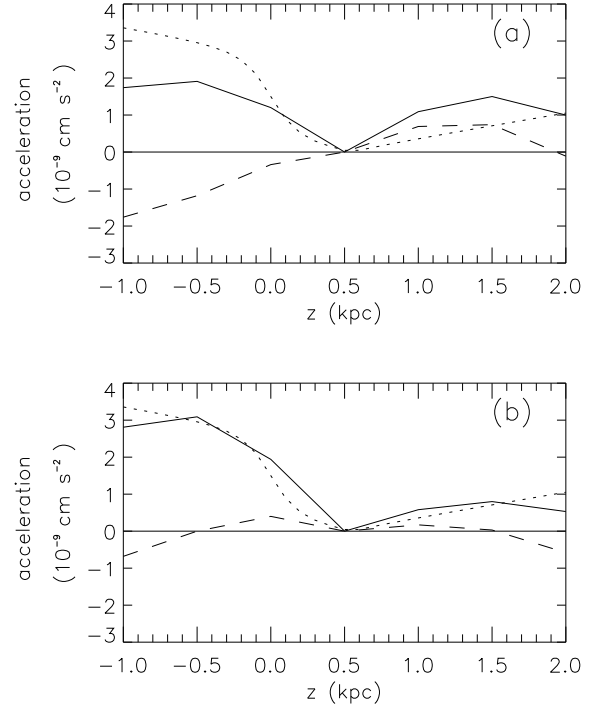


Figure 9. Solid: $|\rho^{-1}\partial P/\partial z|$, the total vertical acceleration due to gravity and the warping force required to maintain the observed HI in hydrostatic equilibrium at $R = 16$ kpc. Dotted: the acceleration $|g + a_0|$ as in Fig. 8. Dashed: a_1 , the difference between the above two. (a): the above with a single velocity dispersion, $u = 11.5 \text{ km s}^{-1}$, and (b): a composite best fit with $u = 8 \text{ km s}^{-1}$ above the shifted midplane and $u = 15 \text{ km s}^{-1}$ below.

equilibrium where approximate equipartition exists between the energy density of the turbulent magnetic field and the turbulent energy density of the gas in its diffuse phases. Models of hydrostatic equilibrium are sensitive to the midplane strength of the regular magnetic field, B_0 .

If $B_0 \simeq 2 \mu\text{G}$, the ISM may be overpressured at $1 \lesssim z \lesssim 4$ kpc (so hydrostatic equilibrium is a poor approximation there), and this can contribute to driving the galactic fountain. The interstellar magnetic field should be coupled more weakly to the molecular clouds than with the other, diffuse gas phases; otherwise, the regular magnetic field strength has a deep, narrow minimum at $z = 0$.

If $B_0 \simeq 4 \mu\text{G}$ then our model gives two-component vertical profiles of both regular, B , and turbulent, b , magnetic fields. The narrower components have scale heights of $h_B \simeq 1$ kpc for the regular magnetic field, $h_b \simeq 0.5$ kpc for the turbulent magnetic field. The more extended components have an approximately constant regular magnetic field strength of $B \simeq 1 \mu\text{G}$ for $2 \lesssim z \lesssim 8$ kpc and $b_0/B_0 = 1.25$ at $z = 0$. The vertical dependence of the degree of linear polarization of synchrotron emission expected from the derived $B(z)$ and $b(z)$, shows a steady increase above $z \simeq 2$ kpc similar to that observed for external edge-on galaxies.

Models with $B_0 \simeq 4 \mu\text{G}$ seem to be simpler and more attractive than those with $B_0 \simeq 2 \mu\text{G}$. The former are consistent with hydrostatic equilibrium maintained at all heights, whereas the overpressure at $1 \lesssim z \lesssim 4$ kpc in the latter mod-

els drives systematic vertical gas flow to the halo at a speed of about 50 km s^{-1} . This counterintuitive conclusion results from a larger contribution of turbulent magnetic fields and cosmic rays to the total pressure required in the latter models for hydrostatic equilibrium at $z \lesssim 1 \text{ kpc}$. We should emphasize that our results with $B_0 \simeq 2 \mu\text{G}$ are only tentative at $z \gtrsim 1 \text{ kpc}$ where our basic assumption of hydrostatic equilibrium does not apply with this value of B_0 .

We have demonstrated in Section 4 that the vertical force acting on the gas in a warped disc should become asymmetric in z , resulting in asymmetry in the gas distribution. By taking the simplest form for the vertical structure of the warping force as a first approximation and assuming hydrostatic equilibrium can be reached, we calculated the expected vertical gas density distribution. The observed warping is produced by an acceleration of $a_0 = 1.5 \times 10^{-9} \text{ cm s}^{-2}$ at $R = 16 \text{ kpc}$. The vertical profiles of neutral hydrogen density in the outer Galaxy (Diplas & Savage 1991) show an asymmetry of the expected form, with the density 0.5 kpc above the shifted midplane a factor of 1.2 higher than the density 0.5 kpc below.

ACKNOWLEDGEMENTS

We are grateful to A. Brandenburg, W. Dobler, K. Ferrière, M. Tagger and E. Zweibel for helpful discussions and to B. Savage for useful comments on his HI data. The comments of the referee, R. Beck, greatly improved the paper. This work was supported by PPARC and the Nuffield Foundation.

REFERENCES

- Badhwar G. D., Stephens S. A., 1977, *ApJ*, 212, 494
 Beck R., 1991, *A&A*, 251, 15
 Beck R., 2001, *Space Sci. Rev.*, Kluwer, Dordrecht, in press (astro-ph/0012402)
 Beck R., Brandenburg A., Moss D., Shukurov A., Sokoloff D., 1996, *ARA&A*, 34, 155
 Berkhuijsen E. M., 1971, *A&A*, 14, 359
 Berkhuijsen E. M., 1999, in M. Ostrowski & R. Schlickeiser, eds, *Plasma Turbulence and Energetic Particles in Astrophysics*. Astron. Obs. Jagellonian Univ., Cracow, p. 61
 Berkhuijsen E. M., Horellou C., Krause M., Poezd A. D., Shukurov A., Sokoloff D. D., 1997, *A&A*, 318, 700
 Beuermann K., Kanbach G., Berkhuijsen E. M., 1985, *A&A*, 153, 17
 Binney J., 1992, *ARA&A*, 30, 51
 Binney J., Tremaine S., 1987, *Galactic dynamics*. Princeton University Press, Princeton
 Bloemen J. B. G. M., 1987, *ApJ*, 322, 694
 Boulares A., Cox D. P., 1990, *ApJ*, 365, 544
 Brandenburg A., Donner K.-J., Moss D., Shukurov A., Sokoloff D. D., Tuominen I., 1992, *A&A*, 259, 453
 Brandenburg A., Donner K.-J., Moss D., Shukurov A., Sokoloff D. D., Tuominen I., 1993, *A&A*, 271, 36
 Brandenburg A., Moss D., Shukurov A., 1995, *MNRAS*, 276, 651
 Bregman J. N., 1980, *ApJ*, 236, 577
 Burn B. J., 1966, *MNRAS*, 133, 67
 Burton W. B., 1988, in Verschuur G. L., Kellermann K. I., eds, *Galactic and Extragalactic Radio Astronomy*. Springer-Verlag, Berlin, p. 296
 Diplas A., Savage B. D., 1991, *ApJ*, 377, 126
 Dumke M., Krause M., Wielebinski R., Klein U., 1995, *A&A*, 302, 691
 Elstner D., Golla G., Rüdiger G., Wielebinski R., 1995, *A&A*, 297, 77
 Ferrière K., 1995, *ApJ*, 441, 281
 Ferrière K., 1998, *ApJ*, 497, 759
 Frick P., Stepanov R., Shukurov A., Sokoloff D., 2001, *MNRAS*, (submitted) (astro-ph/0012459)
 Golla G., Hummel E., 1994, *A&A*, 284, 777
 Habe A., Ikeuchi S., 1980, *Progr. Theor. Phys.*, 64, 1995
 Han J. L., Qiao G. J., 1994, *A&A*, 288, 759
 Hummel E., Lesch H., Wielebinski R., Schlickeiser R., 1988, *A&A*, 197, L29
 Hummel E., Beck R., Dahlem M., 1991, *A&A*, 248, 23
 Kalberla P. M. W., Kerp J., 1998, *A&A*, 339, 745
 Kalberla P. M. W., Westphalen G., Mebold U., Hartmann D., Burton W. B., 1998, *A&A*, 332, L61
 Korpi M. J., Brandenburg A., Shukurov A., Tuominen I., Nordlund Å., 1999, *ApJ*, 514, L99
 Kuijken K., Gilmore G., 1989a, *MNRAS*, 239, 571
 Kuijken K., Gilmore G., 1989b, *MNRAS*, 239, 605
 Kuntz K. D., Danly L., 1996, *ApJ*, 457, 703
 Lockman F. J., Gehman C. S., 1991, *ApJ*, 382, 182
 Lyne A. G., Smith F. G., 1989, *MNRAS*, 237, 533
 Masset F., Tagger M., 1996, *A&A*, 307, 21
 Norman C. A., Ikeuchi S., 1989, *ApJ*, 345, 372
 Parker E. N., 1966, *ApJ*, 145, 811
 Parker E. N., 1979, *Cosmical Magnetic Fields*. Clarendon Press, Oxford
 Phillipps S., Kearsy S., Osborne J. L., Haslam C. G. T., Stoffel H., 1981, *A&A*, 103, 405
 Pietz J., Kerp J., Kalberla P. M. W., Burton W. B., Hartmann D., Mebold U., 1998, *A&A*, 332, 55
 Poezd A., Shukurov A., Sokoloff D., 1993, *MNRAS*, 264, 285
 Rand R. J., Kulkarni S. R., 1989, *ApJ*, 343, 760
 Rand R. J., Lyne A. G., 1994, *MNRAS*, 268, 497
 Reuter H.-P., Klein U., Lesch H., Wielebinski R., Kronberg P. P., 1994, *A&A*, 282, 724 (Erratum: 1994, *A&A*, 213, 287)
 Reynolds R. J., 1990a, in Bowyer S., Leinert C., eds, *The Galactic and Extragalactic Background Radiation*. Kluwer, Dordrecht, p. 157
 Reynolds R. J., 1990b, *ApJ*, 349, L17
 Rohlfs K., 1977, *Lectures on Density Wave Theory*. Springer-Verlag, Berlin
 Rosen A., Bregman J. N., 1995, *ApJ*, 440, 634
 Ruzmaikin A. A., Shukurov A. M., Sokoloff D. D., 1988, *Magnetic Fields of Galaxies*. Kluwer, Dordrecht.
 Shapiro P. R., Field G. B., 1976, *ApJ*, 205, 762
 Shukurov A., 1998, *MNRAS*, 299, L21
 Shukurov A., 1999, in M. Ostrowski & R. Schlickeiser, eds, *Plasma Turbulence and Energetic Particles in Astrophysics*. Astron. Obs. Jagellonian Univ., Cracow, p. 66 (astro-ph/0012444)
 Sofue Y., 1987, *PASJ*, 39, 547
 Sokoloff D. D., Shukurov A., 1990, *Nat*, 347, 51
 Sokoloff D. D., Bykov A. A., Shukurov A., Berkhuijsen E. M., Beck R., Poezd A. D., 1998, *MNRAS*, 299, 189 (Erratum: 1999, *MNRAS*, 303, 207)
 Spoelstra T. A. T., 1984, *A&A*, 135, 238
 Stark A. A., Gammie C. F., Wilson R. W., Bally J., Linke R. A., Heiles C., Hurwitz M., 1991, *ApJS*, 79, 77
 Subramanian K., 1999, *Phys. Rev. Lett.*, 83, 2957
 Wesselius P. R., Fejes I., 1973, *A&A*, 24, 15
 Zweibel E. G., Heiles C., 1997, *Nat*, 385, 131
 Zweibel E. G., McKee C. F., 1995, *ApJ*, 439, 779

This paper has been produced using the Royal Astronomical Society/Blackwell Science L^AT_EX style file.